Frontiers of Information Technology & Electronic Engineering
www.jzus.zju.edu.cn; engineering.cae.cn; www.springerlink.com
ISSN 2095-9184 (print); ISSN 2095-9230 (online)
E-mail: jzus@zju.edu.cn

# Practical fixed-time adaptive fuzzy control of uncertain nonlinear systems with time-varying asymmetric constraints: A unified barrier function-based approach

Zi-xuan Huang†‡1, Huan-qing Wang2, Ben Niu3, Xu-dong Zhao4, Adil M. Ahmad5

[1]*College of Engineering, Bohai University, Jinzhou 121013, Liaoning, China*

[2]*College of Mathematical Science, Bohai University, Jinzhou 121013, Liaoning, China*

[3]*School of Information Science and Engineering, Shandong Normal University, Jinan 250014, Shandong, China*

[4]*Faculty of Electronic Information and Engineering, Dalian University of Technology, Dalian 116024, Liaoning, China*

[5]*Communication Systems and Networks Research Group, Department of Information Technology, Faculty of Computing and Information Technology, King Abdulaziz University, Jeddah, Saudi Arabia*

†E-mail: huangzixuan0301@163.com

Received Jun. 08, 2023; Revision accepted Oct. 13, 2023; Crosschecked



**Abstract:** In this article, a practical fixed-time adaptive fuzzy control strategy is investigated for uncertain nonlinear systems with time-varying asymmetric constraints and input quantization. To overcome the difficulties of designing controllers under the state constraints case, a unified barrier function approach is employed to construct a coordinate transformation that maps the original constrained system to be an equivalent unconstrained one, thus relaxing the time-varying asymmetric constraints upon system states and avoiding the feasibility check condition typically required in the traditional barrier Lyapunov function-based control approach. Meanwhile, the "explosion of complexity" problem in the traditional backstepping approach arising from repeatedly derivatives of virtual controllers is solved by using the command filter method. It is verified via the fixed-time Lyapunov stability criterion that the system output can track a desired signal within a small error range in a predetermined time, and all system states remain in the constraint range. Finally, a simulation example is offered to demonstrate the effectiveness of the proposed strategy.

**Key words:** *unified barrier function, time-varying asymmetric state constraints, fuzzy logic systems, fixed-time control, command filter*

https://doi.org/10.1631/FITEE.2300408 **CLC number:**

## 1 INTRODUCTION

Over the past a few decades, uncertain nonlinear systems that provide a unified mathematical description for most practical systems have received considerable attention from many researchers. Adaptive backstepping technique (Ma et al.,2018; Zhang et al.,2019; Sun et al.,2019), a powerful controller design tool for nonlinear systems, combined with some powerful function approximators (e.g., neural networks or fuzzy logic systems [FLSs]), has been extensively applied to address tracking or the regulation problem for many categories of nonlinear systems, including single-input and single-output nonlinear systems (Wang et al.,2013; Wang et al.,2014), multiple-input and multiple-output nonlinear systems (Chen et al.,2013), large-scale nonlinear systems (Chen and Li,2010), and so on. Note that one disadvantage neglected in current backstepping-

‡ Corresponding author

ORCID: Zi-xuan HUANG, http://orcid.org/0009-0000-5508-1475

based control schemes is the "explosion of complexity" issue, resulting from repeated differentiations of virtual control signals in the design procedure. To address this issue, the authors in (Swaroop et al.,2000) initially presented an adaptive dynamic surface control scheme for strict-feedback nonlinear systems, where a first-order filter was introduced to mitigate the expansion of differential terms of intermediate signals. Following the literature (Swaroop et al.,2000), some modified control strategies free from the issue of "explosion of complexity" have been researched for uncertain nonlinear systems (Sui and Tong,2018; Li and Tong,2016). However, these control schemes were proposed under the framework of asymptotic stability; in other words, they only ensure a system is stable when time tends to infinity, which may limit their application in some practical systems.

As is well known, finite-time control (Bhat and Bernstein,1998) is one of the most effective approaches to rapidly realize the control goal. In comparison with asymptotic stability, finite-time control has a faster convergence rate, shorter response time, and greater anti-disturbance property. Thanks to these advantages, finite-time control has been extensively employed in many real systems, such as robotic manipulator systems (Yu et al.,2005), servo motor systems (Hou et al.,2020), autonomous underwater vehicle systems (Li and Wang,2013), and so on. It should be mentioned that, in the above finite-time control strategies, the settling time of systems is influenced by initial system values, which causes the settling time to be inaccurately calculated. To achieve an exact settling time, a so-called fixed-time control lemma was first presented in (Polyakov,2011), in which the settling time is entirely unrelated to the initial condition, and its upper bound can be calculated by using theoretical methods. Following the work of (Polyakov,2011), many schemes based on fixed-time control have been proposed. (Li et al.,2017) developed a fixed-time backstepping control approach and obtained a semi-globally fixed-time convergence system property. In (Ni et al.,2016), a fast fixed-time sliding mode control approach was developed for power systems, which restrained chaotic systems oscillations. Recently, (Wang and Lai,2020), given the new practical fixed-time stability criterion, offered a new scheme to realize fixed-time control of uncertain strict-feedback nonlinear systems. Compared with the traditional fixed-time stability criterion in (Polyakov,2011), (Li et al.,2017) and (Ni et al.,2016), the one in (Wang and Lai,2020) effectively relaxed the limitations of sufficient condition and extended the applied range of the fixed-time control. Note that the above fixed-time control schemes are suitable only for nonlinear systems whose states are unconstrained, which motivates our current research.



In actual engineering, constraints resulting from physical limitations or safety requirements are frequently encountered, e.g., maximum and minimum chemical reactor temperatures, joint active space for a robotic arm, and so on. During system operation, violating some constraint conditions may lead to system performance degradation or instability, which requires that system states must remain within constrained ranges. To resolve the constraints problem, a barrier Lyapunov function (BLF) approach was first presented in (Tee et al.,2009) and many significant results have been obtained (Tee and Ge,2011; Liu et al.,2023; Liu and Tong,2017; Kim and Yoo,2015; Huang et al.,2023), in which the Lyapunov candidate function can be selected as different barrier function forms, such as logarithmic-type BLFs (Liu and Tong,2017), integral-type BLFs (Kim and Yoo,2015) and tangent-type BLFs (Zhao et al.,2023). Actually, as indicated in the previous literature (Tee and Ge,2011; Tang et al.,2016), only if we search for a series of design parameters satisfying a specific condition, will the BLF-based schemes be available in practice. This restriction is also expressed as the feasibility condition of virtual control signals, namely, the variation range of virtual control signals must stay within certain pre-given constraint areas (Tee and Ge,2011), which results difficulties in some controller designs. If the system state constraint range is small, it is likely that the desired control objective will not be achieved (namely, parameters to meet the feasibility condition do not exist). Recently, another way to address the state constraints problem is the unified barrier function (UBF) approach developed in (Zhao et al.,2020), in which a scalar function was constructed to achieve an equivalent unconstrained model mapped by the original constrained systems; adaptive control of the systems can be realized on the basis of this model. Unlike the current BLF-based methods, the proposed UBF-based method in (Zhao et al.,2020) not only effectively relaxed the constraints upon system states, but also completely removed the feasibility conditions of virtual control signals. It is evident that the UBF-based method has greater application value and development potential than the BLF-based approach. In (Wang et al.,2021), for nonlinear systems with asymmetric state constraints, an adaptive event-triggered control strategy that does not include feasibility conditions has been investigated using the UBF method to handle the state constraints. Subsequently, in (Gao et al.,2022), the UBF approach was extended to interconnected nonlinear systems with dynamic state constraints. On the other hand, communication resource limits for control signal transmissions should be considered during the design process, which can prevent the loss of available information. In (Shi et al.,2020), a hysteresis quantizer was constructed that reduced the communication burden by generating the input signal within a limited set and had an extra quantification level to alleviate the high-frequency chattering in the other quantizers. As far as we know, for systems with state constraints and communication resource limitations, how to make the output of the system track the desired signal at a predetermined time without violating the state constraints is still a meaningful problem in the control field.

Enlightened by the aforementioned discussions, a UBF-based practical fixed-time adaptive fuzzy control approach is proposed in this article for uncertain nonlinear systems with input quantization and time-varying asymmetric constraints. In comparison with existing results, the primary differences and contributions of this research are summarized in the following three points:

(1) The proposed control approach can ensure the practical fixed-time stability of a class of uncertain nonlinear systems, while the settling time of the system is entirely unrelated to initial values of system states and its upper bound also can be obtained.

(2) Different from the BLF-based schemes (Tee and Ge,2011; Li,2020; Tang et al.,2016), a new UBF method is used to overcome the difficulties caused by state constraints for designing controllers. This function constructs an unconstrained system model of the original constrained system, so the restrictions on system states are relaxed and the feasibility conditions of virtual control signals are completely eliminated.

(3) A modified hysteretic quantizer is constructed to save communication resources in practical applications, and has extra quantization levels to alleviate the high-frequency chatter.

This article is organized as follows: **Section** 2 exhibits some problem formulations and necessary preliminaries for the investigated system. The fixed-time controller design process and the system stability analysis procedure are shown in **Section** 3. In **Section** 4, a simulation result is provided to verify the availability of the proposed method. Some conclusions are summarized in **Section** 5.

### 1.1 Notation

$R$ denotes the compact set of real numbers. $R_+$ represents the compact set of positive real numbers. $R^j$ expresses the $j$-dimensional Euclidean space. $U_i$ and $U_d$ stand for the constrained region of system state $x_i$ and desired signal $y_d$, respectively. $\Theta$ indicates the mathematical set. $x^T$ means the transpose of vector $x$. $|\cdot|$ is the absolute value of $(\cdot)$. $\|\cdot\|$ signifies the standard 2-form of $(\cdot)$. $\Xi_{il}$ and $\Xi_{ih}$ are the compact set of constraint functions $k_{il}(t)$ and $k_{ih}(t)$, respectively.

## 2 PROBLEM FORMULATION AND PRELIMINARIES

### 2.1 System Descriptions and Lemmas

Taking the following uncertain nonlinear systems into account:

$$\begin{cases} \dot{x}_i = x_{i+1} + f_i\left(\bar{x}_n\right), \\ \dot{x}_n = g\left(\bar{x}_n\right) q\left(u\right) + f_n\left(\bar{x}_n\right), \\ y = x_1, \qquad i = 1, \ldots, n-1, \end{cases} \tag{1}$$

where $\bar{x}_n = [x_1, x_2, \ldots, x_n]^T \in R^n$ denotes the system state vector, and $y$ and $q(u)$ indicate the system output and the quantized input, respectively. $g(\bar{x}_n)$ and $f(\bar{x}_n)$ are the unknown nonlinear functions. In addition, the system state $x_i$ is restricted by the time-varying asymmetric constraint, which is described as follows:

$$\begin{aligned} x_i \in U_i := \big\{(t, x_i) \in (R_+ \times R) | \\ k_{il}\left(t\right) < x_i < k_{ih}\left(t\right), k_{il} \in R, k_{ih} \in R\big\}. \end{aligned} \tag{2}$$

**Remark 1.** $k_{il}(t)$ and $k_{ih}(t)$ are first-order differentiable functions defined in set $\Theta := \big\{k_{il}(t)\colon R_+ \to R,\ k_{ih}(t)\colon R_+ \to R\big\}$, and their initial conditions

$k_{il}(0)$ and $k_{ih}(0)$, respectively, satisfy $k_{il}(0) \in \Xi_{il}$ and $k_{ih}(0) \in \Xi_{ih}$. Also, $k_{il}(t)$ and $k_{ih}(t)$ have the relation $k_{il}(t) < k_{ih}(t)$.

The hysteresis quantizer is shown as follows,

$$q(u) = \begin{cases} u_i sgn(u), & \frac{u_i}{1+\delta} < |u| \le u_i, \dot{u} < 0 \text{ or} \\ & u_i < |u| \le \frac{u_i}{1-\delta}, \dot{u} > 0 \\ u_i(1+\delta), & u_i < |u| \le \frac{u_i}{1-\delta}, \dot{u} < 0 \text{ or} \\ & \frac{u_i}{1-\delta} < |u| \le \frac{u_i(1+\delta)}{1-\delta}, \dot{u} > 0 \\ 0, & 0 \le |u| < \frac{u_{min}}{1+\delta}, \dot{u} < 0 \text{ or} \\ & \frac{u_{min}}{1+\delta} \le u \le u_{min}, \dot{u} > 0 \\ q(u(t^-)), & \text{other} \end{cases} \quad (3)$$

where $\delta = \frac{1-\lambda}{1+\lambda}$, and $u_i = \lambda^{1-i} u_{\min}$, $(i = 1, 2...)$, with $u_{\min} > 0$ deciding the range of the dead zone for $q(u)$. The parameter $\lambda$ satisfying $0 < \lambda < 1$ denotes the measure of quantization density. **Fig**. 1 displays the map of the hysteresis quantizer Eq.(3). According to (Guo et al.,2023), the quantized input can be disassembled as two parts, namely, $q(u) = G(u)u + D(t)$, where $0 < 1 - \delta \le G(u) \le 1 + \delta$ and $|D(t)| \le u_{\min}$.

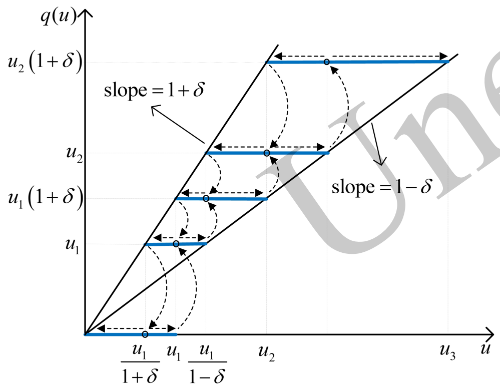


**Fig. 1 The map of the hysteresis quantizer** $q(u)$

**Remark 2.** The hysteresis quantizer can be classified as a non-uniform quantizer owing to its unequal quantization level. This quantizer is the coarsest quantizer, which minimizes the average speed of communication cases and is simple to realize in practice. Different from other quantizers, the hysteresis quantizer has extra quantization levels to mitigate undesired chattering.

The control goal of this technical note is to design a practical fixed-time adaptive controller for the considered system (1), which makes the system output $y$ follow the desired signal $y_d$ and all states remain within the time-varying asymmetric state constraints. To achieve this goal, we give some common assumptions and lemmas as follows.

**Assumption 1.** The function $g(\overline{x}_n)$ is unknown and bounded, and there exist positive constants $\overline{g}$ and $\underline{g}$, which makes the inequality $0 < \underline{g} \le g(\overline{x}_n) \le \overline{g} < \infty$ hold.

**Assumption 2.** The desired signal $y_d$ is defined in set $U_d := \{(t, y_d) \in [0, \infty) \times R : k_{dl}(t) \le y_d \le k_{dh}(t)\}$, and its derivatives up to second order are bounded and known. Meanwhile, there exist positive constants $\overline{\xi}$ and $\underline{\xi}$ such that inequalities $k_{1h}(t) - k_{dh}(t) \ge \overline{\xi} > 0$ and $k_{dl}(t) - k_{1l}(t) \ge \underline{\xi} > 0$ hold (i.e., $U_d \subset U_1$).

**Remark 3. Assumption 1** indicates the boundedness of control gain functions, and it is reasonable to require that $g(\bar{x}_n)$ is away from zero to make the system controllable. Moreover, in practical cases, the control gain is not always a constant.

**Lemma 1** (see Wang and Lai,2020)**.** For a nonlinear system, if there exists a positive definite function $V(x)$ that satisfies

$$\begin{cases} \dot{V}(x) \le -c_1 V^p(x) - c_2 V^q(x) + b, \\ \beta(\|x\|) \le V(x) \le \alpha(\|x\|), \end{cases} \quad (4)$$

where $c_1, c_2 > 0$, $q > 1$, $0 < p < 1$, $b > 0$ and it meets $b < min\{(1-\xi)c_1, (1-\xi)c_2\}$ $(0 < \xi < 1)$, and $\beta$, $\alpha$ are $\kappa_\infty -$ functions, then we can deduce that the system is practical fixed-time stable, and the upper bound of the settling time $T_m$ can be computed by the formula $T \le T_m = \frac{1}{\xi c_1(1-p)} + \frac{1}{\xi c_2(q-1)}$.

**Lemma 2** (see Li,2019)**.** For real variables $x, s$, and arbitrary positive constants $a$, $b$ ,$\omega$, there exists that $|s|^a |x|^b \le \frac{a}{a+b}\omega |s|^{a+b} + \frac{b}{a+b}\omega^{-\frac{a}{b}} |x|^{a+b}$.

**Lemma 3** (see Zuo et al.,2017)**.** Suppose that the variable $s_i \ge 0$ and two positive constants $0 < r < 1$, $m > 1$, then we can deduce that $\left(\sum\limits_{i=1}^{n} s_i\right)^r \le \sum\limits_{i=1}^{n} s_i^r$ and $\left(\sum\limits_{i=1}^{n} s_i\right)^m \le n^{m-1} \sum\limits_{i=1}^{n} s_i^m$.

**Lemma 4** (see Huang et al.,2018)**.** If the positive definite function $V(t)$ satisfies $V(t) \le \sum\limits_{j=1}^{n} \int_0^t \left(k_j(N_j(v_j) - 1)\ \dot{v}_j\ (\tau)\right) d\tau + c$, where $N_j(v_j)$ is a Nussbaum-type function and $c$, $k_j$ are positive constants, then we can infer that $V(t)$, $\sum\limits_{j=1}^{n} \int_0^t (k_j(N_j(v_j) - 1)\dot{v}_j(\tau))d\tau$ and $v_j$ are bounded.

**Lemma 5** (see Xu et al.,2022)**.** Assume that $s \ge 0$ is a real number. We have that $s \le s^n + s^m$, where $0 < n < 1$ and $m > 1$ are constants.

### 2.2 Fuzzy Logic Systems

As we know, FLSs can approximate the unknown nonlinear function to arbitrary accuracy. According to (Zhao et al.,2023), the unknown nonlinear function $f(X)$ can be represented as $f(X) = W^T S(X) + \delta(X)$, where $X \in R^m$ indicates the input vector, and $W = [w_1,\ w_2,\ ...,\ w_l]^T$ represents the optimal weight vector. $\delta(X)$ expresses the approximation error and satisfies $||\delta|| \leq \varepsilon$ with $\varepsilon$ being a positive constant. $S(X) = [\zeta_1(X), \zeta_2(X), ..., \zeta_l(X)]^T$ indicates the basis function vector, and $\zeta_i(X)$ is chosen as a Gaussian function, which is described as

$$\zeta_i(X) = exp\left(-\frac{(X-\mu_i)^T(X-\mu_i)}{\sigma^2}\right), 1 \leq i \leq l, \quad (5)$$

where $l$ expresses the number of fuzzy rules, $\mu_i = [\mu_{i1}, \mu_{i2}, ..., \mu_{im}]^T$ denotes the center vector, and $\sigma$ stands for the width of the Gaussian function.

### 2.3 Unified Barrier Function

In this subsection, we will present some properties of the UBF. The definition of the UBF is as follows:

**Definition 1** (Zhao et al.,2020). If the scalar function $\zeta(x)$ $(x \in U)$ satisfies the following conditions:

(1) The state constraints are disposed without modifying the function structure.

(2) It shows a performance that $\zeta \to \pm\infty$ when $x$ is close to the boundary of $U$, and there exists a bounded constant $c$ such that $\zeta \leq c$ for $\forall x \in U' \subset U$ under initial condition $x(0) \in U$, where $U'$ is a closed interval; then the scalar function $\zeta$ is a UBF.

Considering **Definition** 1, by defining $\zeta_{i,1} = \frac{\overline{k}_{il} - k_{il} + k_{ih} - \underline{k}_{ih}}{(x_i - k_{il})(k_{ih} - x_i)}$ and $\zeta_{i,2} = \frac{k_{il}\underline{k}_{ih} - \overline{k}_{il}k_{ih}}{(x_i - k_{il})(k_{ih} - x_i)}$, the UBF of $x_i$ can be constructed as

$$\zeta_i = \zeta_{i,1} x_i + \zeta_{i,2}, \quad (6)$$

where $\overline{k}_{il}$ and $\underline{k}_{ih}$ are constants satisfying $k_{il}(t) < \overline{k}_{il}$ and $\underline{k}_{ih} < k_{ih}(t)$. Then, constructing $\zeta_{i,3} = \frac{\zeta_{i,2}}{\zeta_{i,1}}$, the system state $x_i$ can be reformulated as

$$x_i = \frac{\zeta_i}{\zeta_{i,1}} - \zeta_{i,3}. \quad (7)$$

In addition, from (Zhao et al.,2020), we can obtain the following property for $\zeta_i$

$$\begin{cases} \zeta_i \to -\infty \text{ when } x_i \to k_{il}^{+}(t), \\ \zeta_i \to +\infty \text{ when } x_i \to k_{ih}^{-}(t). \end{cases} \quad (8)$$

The constructed UBF $\zeta_i$ contributes to creating an unconstrained equivalent model later and prevent system states from violating the time-varying asymmetric constraints. The closed-loop control structure diagram of the controlled system is given in **Fig.** 2.

## 3 MAIN RESULTS

In this section, we first need to construct an unconstrained equivalent model for the control system (1). Second, on the basis of this model, a practical fixed time adaptive controller is established by applying FLSs and dynamic surface control methods. Finally, the stability analysis outcomes are offered to verify the stability of systems.

### 3.1 Design of an Equivalent Unconstrained Model

In this subsection, to facilitate the subsequent formula derivation, we need to construct an unconstrained equivalent model of the original constrained system. This process is described as follows in detail. First, taking the derivative of $\dot{\zeta}_i$ produces

$$\dot{\zeta}_i = \eta_{i,1}\dot{x}_i + \eta_{i,2}, \quad (9)$$

where $\eta_{i,1} = \frac{\overline{k}_{il} - k_{il}}{(x_i - k_{il})^2} + \frac{k_{ih} - \underline{k}_{ih}}{(k_{ih} - x_i)^2}$ and $\eta_{i,2} = \frac{(x_i - \overline{k}_{il})\dot{k}_{il}}{(x_i - k_{il})^2} + \frac{\dot{k}_{ih}(x_i - \underline{k}_{ih})}{(k_{ih} - x_i)^2}$. Then, integrating the system model (1) with Eq.(9), we can arrive at an equivalent model as follows:

$$\begin{cases} \dot{\zeta}_i = \eta_{i,1}(f_i(\overline{x}_n) + x_{i+1}) + \eta_{i,2}, \\ \dot{\zeta}_n = \eta_{n,1}(f_n(\overline{x}_n) + gq(u)) + \eta_{n,2}. \end{cases} \quad (10)$$

Substituting Eq.(7) into Eq.(10), the equivalent model becomes

$$\begin{cases} \dot{\zeta}_i = \eta_{i,1}(f_i(\overline{x}_n) + \frac{\zeta_{i+1}}{\zeta_{i+1,1}} - \zeta_{i+1,3}) + \eta_{i,2}, \\ \dot{\zeta}_n = \eta_{n,1}(f_n(\overline{x}_n) + gq(u)) + \eta_{n,2}, \end{cases} \quad (11)$$

where $\zeta_i$ is the new state variable without state constraints. From this, for any initial condition $x_i(0) \in U_i$, if $\zeta_i$ can be made bounded, then the state $x_i$ maintains in the region $U_i$, namely, states remain within a pre-determined constraints interval. It should be pointed out that $\zeta_{i,1}$, $\zeta_{i,2}$, $\zeta_{i,3}$, $\eta_{i,1}$ and $\eta_{i,2}$ are well defined in sets $U_i$. Here, the unconstrained equivalent model is constructed.

### 3.2 Controller Design

In this subsection, we will apply the backstepping technique to construct the practical fixed time

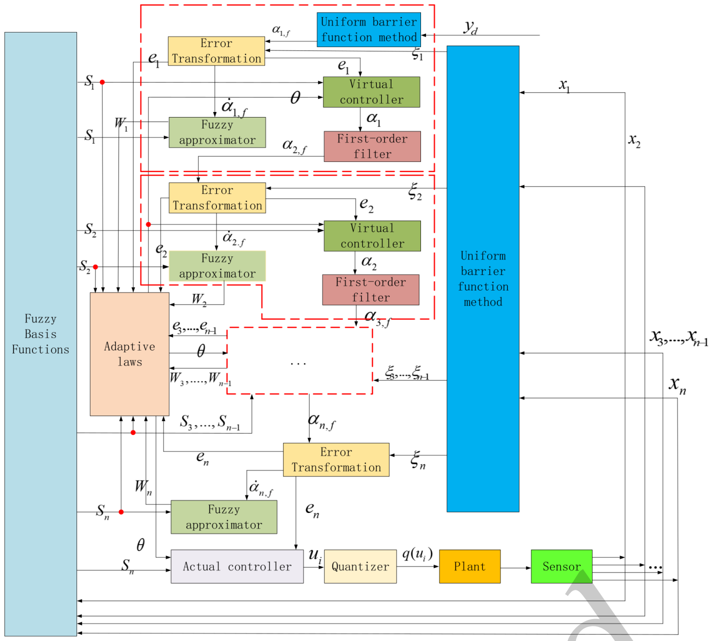


**Fig. 2 The closed-loop control structure diagram of the controlled system.**



adaptive controller. The main design procedure can be broken down into n steps, whose details are shown later. To relax the time-varying asymmetric constraint and to eliminate the feasibility condition, a coordinate transformation based on the converted model (11) is introduced

$$\begin{cases} e_1 = \zeta_1 - \alpha_{1,f}, \\ e_i = \zeta_i - \alpha_{i,f}, \end{cases} \tag{12}$$

where $\alpha_{1,f} = \frac{y_d - \bar{k}_{1l}}{y_d - k_{1l}} + \frac{y_d - k_{1h}}{k_{1h} - y_d}$, and $\alpha_{i,f}$ is the output signal of first-order filter.

Define the first-order filter as

$$\tau_i \dot{\alpha}_{i,f} + \alpha_{i,f} = \alpha_{i-1}, i = 2, 3, \ \dots\ n, \tag{13}$$

where $\tau_i > 0$ is a constant, and the virtual control signal $\alpha_{i-1}$ is the input signal of the first-order filter.

**Step 1**: By establishing the Lyapunov candidate function as $V_1 = \frac{1}{2}e_1^2 + \frac{1}{2\gamma}\tilde{\theta}^2$ with $\gamma > 0$ being a design parameter, and calculating the derivative of $e_1$

$$\begin{aligned} \dot{e}_1 = &\eta_{1,1}(f_1 + \tfrac{e_2}{\zeta_{2,1}} + \tfrac{\alpha_1}{\zeta_{2,1}} - \zeta_{2,3}) \\ &+\eta_{1,1}(\tfrac{\alpha_{2,f}}{\zeta_{2,1}} - \tfrac{\alpha_1}{\zeta_{2,1}}) + \eta_{1,2} - \dot{\alpha}_{1,f}, \end{aligned} \tag{14}$$

then, taking the derivative of $V_1$, there exists

$$\begin{aligned} \dot{V}_1 = &e_1(\tfrac{\eta_{1,1}}{\zeta_{2,1}}e_2 + \tfrac{\eta_{1,1}}{\zeta_{2,1}}\alpha_1 - \eta_{1,1}\zeta_{2,3} + \eta_{1,2}) \\ &+e_1\tfrac{\eta_{1,1}}{\zeta_{2,1}}e_{2,\alpha} + e_1(\eta_{1,1}f_1 - \dot{\alpha}_{1,f}) - \tfrac{1}{\gamma}\tilde{\theta}\dot{\hat{\theta}}, \end{aligned} \tag{15}$$

where $e_{2,\alpha} = \alpha_{2,f} - \alpha_1$ denotes the filtering error. Define $h_1(Z_1) = \eta_{1,1}f_1 - \dot{\alpha}_{1,f}$ with $Z_1 = [\bar{x}_n, \dot{\alpha}_{1,f}]^T$ being the input of FLSs. Because $h_1(Z_1)$ includes the unknown uncertainties, $h_1(Z_1)$ can be expressed within the approximation error $\delta_1(Z_1)$ as FLSs of the following form:

$$h_1(Z_1) = W_1^T S_1(Z_1) + \delta_1(Z_1), \tag{16}$$

where $||\delta_1(Z_1)|| \le \varepsilon_1$ and $\varepsilon_1 > 0$ is a constant. With the assistance of the Young's inequality, there exists

$$\begin{aligned} e_1 h_1(Z_1) = &e_1(W_1^T S_1(Z_1) + \delta_1(Z_1)) \\ \le &\tfrac{1}{2{a_1}^2}e_1^2\theta S_1^T S_1 + \tfrac{1}{2}a_1^2 \\ &+k_1 e_1^2 + \tfrac{1}{4k_1}\varepsilon_1^2, \end{aligned} \tag{17}$$

$$\frac{\eta_{1,1}}{\zeta_{2,1}}e_{2,\alpha}e_1 \le \frac{1}{2}e_{2,\alpha}^2 + \frac{1}{2}e_1^2(\frac{\eta_{1,1}}{\zeta_{2,1}})^2, \tag{18}$$

where $a_1 > 0$ is a constant, and $\theta = \max\{\ ||W_1||^2, ||W_2||^2, \dots, ||W_n||^2\}$ denotes the adaptive parameter. It is immediate from Eqs(15), (17), and (18) that

$$\begin{aligned} \dot{V}_1 \le &e_1(\tfrac{\eta_{1,1}}{\zeta_{2,1}}e_2 + \tfrac{\eta_{1,1}}{\zeta_{2,1}}\alpha_1 - \eta_{1,1}\zeta_{2,3} + \eta_{1,2}) \\ &+\tfrac{1}{2}e_{2,\alpha}^2 + \tfrac{1}{2}e_1^2(\tfrac{\eta_{1,1}}{\zeta_{2,1}})^2 + \tfrac{1}{2}{a_1}^2 + k_1{e_1}^2 \\ &+\tfrac{1}{2a_1^2}{e_1}^2\theta {S_1}^T S_1 + \tfrac{1}{4k_1}{\varepsilon_1}^2 - \tfrac{1}{\gamma}\tilde{\theta}\dot{\hat{\theta}}, \end{aligned} \tag{19}$$

where $\hat{\theta}$ and $\tilde{\theta}$ are, respectively, the estimation and the estimation error of $\theta$.

If the virtual control law is constructed as

$$\begin{aligned}\alpha_1 = &-\tfrac{\zeta_{2,1}}{\eta_{1,1}}k_1e_1 - \tfrac{\zeta_{2,1}}{\eta_{1,1}}\eta_{1,2} - \tfrac{\eta_{1,1}}{2\zeta_{2,1}}e_1 \\ &-\tfrac{\zeta_{2,1}}{\eta_{1,1}}c_{1,1}e_1^{2p-1} - \tfrac{\zeta_{2,1}}{\eta_{1,1}}c_{1,2}e_1^{2q-1} \\ &-\tfrac{\zeta_{2,1}}{\eta_{1,1}}\tfrac{1}{2a_1^2}e_1\hat{\theta}{S_1}^TS_1 + \zeta_{2,1}\zeta_{2,3},\end{aligned} \tag{20}$$

where $c_{1,1} > 0$ and $c_{1,2} > 0$ are design parameters, then $\dot{V}_1$ satisfies

$$\begin{aligned}\dot{V}_1 \leq &-c_{1,1}e_1^{2p} - c_{1,2}e_1^{2q} - \tfrac{1}{\gamma}\tilde{\theta}\dot{\hat{\theta}} + \tfrac{\eta_{1,1}}{\zeta_{2,1}}e_1e_2 \\ &+\tfrac{1}{2a_1^2}e_1^2\tilde{\theta}S_1^TS_1 + \tfrac{1}{2}a_1^2 + \tfrac{1}{4k_1}\varepsilon_1^2 + \tfrac{1}{2}e_{2,\alpha}^2.\end{aligned} \tag{21}$$

**Step i ($\mathbf{2 \leq i \leq n-1}$)**: By choosing the **i-th** Lyapunov candidate function as $V_i = V_{i-1} + \frac{1}{2}e_i^2$, and calculating the derivative of $e_i$

$$\begin{aligned}\dot{e}_i = &\eta_{i,1}\big(\tfrac{e_{i+1}}{\zeta_{i+1,1}} + \tfrac{e_{i+1,\alpha}}{\zeta_{i+1,1}} + \tfrac{\alpha_i}{\zeta_{i+1,1}} - \zeta_{i+1,3}\big) \\ &+\eta_{i,2} + \eta_{i,1}f_i - \dot{\alpha}_{i,f},\end{aligned} \tag{22}$$

then, taking the time-derivative of $V_i$ results in

$$\begin{aligned}\dot{V}_i = &\dot{V}_{i-1} + e_i(\eta_{i,1}f_i - \dot{\alpha}_{i,f}) + e_i\big(\tfrac{\eta_{i,1}e_{i+1}}{\zeta_{i+1,1}} \\ &+\tfrac{\eta_{i,1}e_{i+1,\alpha}}{\zeta_{i+1,1}} + \tfrac{\eta_{i,1}\alpha_i}{\zeta_{i+1,1}} - \eta_{i,1}\zeta_{i+1,3} + \eta_{i,2}\big).\end{aligned} \tag{23}$$

where $e_{i+1,\alpha} = \alpha_{i+1,f} - \alpha_i$ is the filtering error. As with **Step 1**, we define a function $h_i(Z_i) = \eta_{i,1}f_i - \dot{\alpha}_{i,f}$, and its input is $Z_i = [\bar{x}_n,\ \dot{\alpha}_{i,f}]^T$. The function $h_i(Z_i)$ can be approximated by FLSs, which is expressed as $h_i(Z_i) = {W_i}^TS_i(Z_i) + \delta_i(Z_i)$ and $||\delta_i(Z_i)|| \leq \varepsilon_i$. By utilizing Young's inequality, it can be deduced that

$$\begin{aligned}e_ih_i(Z_i) &= e_i({W_i}^TS_i(Z_i) + \delta_1(Z_i)) \\ &\leq \tfrac{1}{2a_i^2}{e_i}^2\theta{S_i}^TS_i + \tfrac{1}{2}{a_i}^2 \\ &\quad +k_i{e_i}^2 + \tfrac{1}{4k_i}{\varepsilon_i}^2,\end{aligned} \tag{24}$$

$$\frac{\eta_{i,1}}{\zeta_{i+1,1}}e_{i+1,\alpha}e_i \leq \frac{1}{2}e_{i+1,a}^2 + \frac{1}{2}e_i^2\Big(\frac{\eta_{i,1}}{\zeta_{i+1,1}}\Big)^2, \tag{25}$$

where $a_i > 0$ is a constant. Considering Eqs(24) and (25), one has

$$\begin{aligned}\dot{V}_i \leq &\dot{V}_{i-1} + \tfrac{1}{2}a_i^2 + \tfrac{1}{4k_i}\varepsilon_i^2 + \tfrac{1}{2}e_{i+1,a}^2 + k_ie_i^2 \\ &+\tfrac{1}{2}e_i^2\big(\tfrac{\eta_{i,1}}{\zeta_{i+1,1}}\big)^2 + \tfrac{1}{2a_i^2}e_i^2\theta S_i^TS_i + e_i\big(\eta_{i,2} \\ &+\tfrac{\eta_{i,1}}{\zeta_{i+1,1}}e_{i+1} - \eta_{i,1}\zeta_{i+1,3} + \tfrac{\eta_{i,1}}{\zeta_{i+1,1}}\alpha_i\big).\end{aligned} \tag{26}$$

Establish the virtual control law as

$$\begin{aligned}\alpha_i = &-\tfrac{\zeta_{i+1,1}}{\eta_{i,1}}\big(c_{i,1}e_i^{2p-1} + c_{i,2}e_i^{2q-1} + \eta_{i,2} \\ &+\tfrac{\eta_{i-1,1}}{\zeta_{i,1}}e_{i-1} + k_ie_i + \tfrac{1}{2a_i^2}e_i\hat{\theta}{S_i}^TS_i\big) \\ &-\tfrac{\eta_{i,1}}{2\zeta_{i+1,1}}e_i + \zeta_{i+1,1}\zeta_{i+1,3},\end{aligned} \tag{27}$$

where $c_{i,1}$ and $c_{i,2}$ are positive design parameters. By combining Eqs(26) and (27), $\dot{V}_i$ can turn into

$$\begin{aligned}\dot{V}_i \leq &\dot{V}_{i-1} - c_{i,1}e_i^{2p} - c_{i,2}{e_i}^{2q} - k_ie_i^2 \\ &-\tfrac{1}{2}e_i^2\big(\tfrac{\eta_{i,1}}{\zeta_{i+1,1}}\big)^2 + \tfrac{\eta_{i,1}}{\zeta_{i+1,1}}e_ie_{i+1} + \tfrac{1}{2}a_i^2 \\ &+\tfrac{1}{4k_i}\varepsilon_i^2 + k_ie_i^2 + \tfrac{1}{2}e_{i+1,a}^2 + \tfrac{1}{2}e_i^2\big(\tfrac{\eta_{i,1}}{\zeta_{i+1,1}}\big)^2 \\ &-\tfrac{\eta_{i-1,1}}{\zeta_{i,1}}e_ie_{i-1} + \tfrac{1}{2a_i^2}e_i^2\tilde{\theta}{S_i}^TS_i \\ \leq &-\sum_{j=1}^{i}(c_{j,1}e_j^{2p} + c_{j,2}e_j^{2q}) + \tfrac{\eta_{i,1}}{\zeta_{i+1,1}}e_ie_{i+1} \\ &-\tfrac{\tilde{\theta}}{\gamma}\big(\dot{\hat{\theta}} - \sum_{j=1}^{i}\gamma\tfrac{1}{2a_j^2}e_j^2S_j^TS_j\big) \\ &+\sum_{j=1}^{i}\big(\tfrac{1}{2}a_j^2 + \tfrac{1}{4k_j}\varepsilon_j^2 + \tfrac{1}{2}e_{j+1,a}^2\big).\end{aligned} \tag{28}$$

**Step n**: In this step, a practical fixed time adaptive controller will be constructed for the considered systems (1). In view of the communication resources of the system, a hysteresis quantizer described by the model (3) will be used. Build the **n-th** Lyapunov candidate function as $V_n = V_{n-1} + \frac{1}{2}e_n^2$. Computing the derivative of $e_n$ yields

$$\dot{e}_n = \eta_{n,1}(f_n + gq(u)) + \eta_{n,2} - \dot{\alpha}_{n,f}. \tag{29}$$

Due to $q(u) = G(u)u + D(t)$, $\dot{e}_n$ can be shown as

$$\begin{aligned}\dot{e}_n = &\eta_{n,1}(f_n + gG(u)u) \\ &+\eta_{n,2} - \dot{\alpha}_{n,f} + \eta_{n,1}gD(t).\end{aligned} \tag{30}$$

Taking the time-derivative of $V_n$, we arrive at

$$\begin{aligned}\dot{V}_n = &\dot{V}_{n-1} + e_n(\eta_{n,1}gG(u)u + \eta_{n,2}) \\ &+e_n(\eta_{n,1}f_n - \dot{\alpha}_{n,f}) + e_n\eta_{n,1}gD(t).\end{aligned} \tag{31}$$

Similarly, define the function $h_n(Z_n) = \eta_{n,1}f_n - \dot{\alpha}_{n,f}$ with the variable $Z_n = [\bar{x}_n,\ \dot{\alpha}_{n,f}]^T$ being the input signal. The function $h_n(Z_n)$ can be approached by FLSs, which is represented as $h_n(Z_n) = {W_n}^TS_n(Z_n) + \delta_n(Z_n)$ and $||\delta_n(Z_n)|| \leq \varepsilon_n$. As in the cases of Eqs(24) and (25), the following inequality holds:

$$\begin{aligned}e_nh_n(Z_n) &= e_n(W_n^TS_n(Z_n) + \delta_n(Z_n)) \\ &\leq \tfrac{1}{2a_n^2}e_n^2\theta S_n^TS_n + \tfrac{1}{2}a_n^2 \\ &\quad +k_ne_n^2 + \tfrac{1}{4k_n}\varepsilon_n^2,\end{aligned} \tag{32}$$

Based on **Assumption 1**, there exists

$$\eta_{n,1}gD(t)e_n \leq \tfrac{1}{2}{\eta_{n,1}}^2{e_n}^2\bar{g}^2 + \tfrac{1}{2}{u_{min}}^2, \tag{33}$$

where $a_n > 0$ is a positive parameter.

It is clear from Eqs(31)-(33) that

$$\begin{aligned}\dot{V}_n \leq& \dot{V}_{n-1} + e_n(\eta_{n,1} g G(u)u + \eta_{n,2}) \\ &+ \tfrac{1}{2a_n^2} e_n^2 \theta S_n{}^T S_n + \tfrac{1}{2} a_n^2 + k_n e_n^2 \\ &+ \tfrac{1}{4k_n} \varepsilon_n^2 + \tfrac{1}{2} \eta_{n,1}{}^2 e_n{}^2 \bar{g}^2 + \tfrac{1}{2} u_{min}{}^2.\end{aligned} \quad (34)$$

In light of **Assumption 1**, the virtual controller is established as

$$\begin{aligned}u =& \tfrac{1}{\eta_{n,1} \underline{g}(1-\delta)}(-c_{n,1} e_n{}^{2p-1} - c_{n,2} e_n^{2q-1} \\ &- \tfrac{\eta_{n-1,1}}{\zeta_{n,1}} e_{n-1} - k_n e_n - \tfrac{1}{2a_n^2} e_n \hat{\theta} S_n^T S_n \\ &- \eta_{n,2} - \tfrac{1}{2} \eta_{n,1}{}^2 e_n \bar{g}^2).\end{aligned} \quad (35)$$

Considering the relation $0 < 1-\delta \leq G(u) \leq 1+\delta$ and **Assumption 1** , we can deduce the following inequality

$$\begin{aligned}G(u)u \leq& \tfrac{1}{\eta_{n,1} \underline{g}}(-c_{n,1} e_n{}^{2p-1} - c_{n,2} e_n^{2q-1} \\ &- \tfrac{\eta_{n-1,1}}{\zeta_{n,1}} e_{n-1} - \tfrac{1}{2a_n^2} e_n \hat{\theta} S_n{}^T S_n \\ &- k_n e_n - \eta_{n,2} - \tfrac{1}{2} \eta_{n,1}{}^2 e_n \bar{g}^2).\end{aligned} \quad (36)$$

Substituting Eq.(36) into Eq.(34) results in

$$\begin{aligned}\dot{V}_n \leq& \dot{V}_{n-1} - c_{n,1} e_n^{2p} - c_{n,2} e_n^{2q} - k_n e_n^2 \\ &- \tfrac{\eta_{n-1,1}}{\zeta_{n,1}} e_n e_{n-1} + \tfrac{1}{2a_n^2} v_n^2 \tilde{\theta} S_n^T S_n \\ &+ \tfrac{1}{2} a_n^2 + \tfrac{1}{4k_n} \varepsilon_n^2 + k_n e_n^2 + \tfrac{1}{2} u_{min}{}^2 \\ \leq& - \sum_{i=1}^{n} (c_{i,1} e_i^{2p} + c_{i,2} e_i^{2q}) + \sum_{i=2}^{n} \tfrac{1}{2} e_{i,a}^2 \\ &+ \sum_{i=1}^{n} (\tfrac{1}{2} a_i^2 + \tfrac{1}{4k_i} \varepsilon_i^2) + \tfrac{1}{2} u_{min}{}^2 \\ &- \tfrac{\tilde{\theta}}{\gamma}(\dot{\hat{\theta}} - \sum_{i=1}^{n} \gamma \tfrac{1}{2a_i^2} e_i^2 S_i^T S_i).\end{aligned} \quad (37)$$

By constructing the adaptive law as

$$\dot{\hat{\theta}} = \sum_{i=1}^{n} \gamma \tfrac{1}{2a_i^2} e_i^2 S_i^T S_i - \sigma_1 \hat{\theta} - \sigma_2 \hat{\theta}^{2q-1}, \quad (38)$$

we have

$$\begin{aligned}\dot{V}_n \leq& - \sum_{i=1}^{n} (c_{i,1} e_i^{2p} + c_{i,2} e_i^{2q}) \\ &+ \tfrac{\sigma_1}{\gamma} \tilde{\theta} \hat{\theta} + \tfrac{\sigma_2}{\gamma} \tilde{\theta} \hat{\theta}^{2q} + b_n,\end{aligned} \quad (39)$$

where $b_n = \sum_{i=1}^{n} (\frac{1}{2} a_i^2 + \frac{1}{4k_i} \varepsilon_i^2) + \sum_{i=2}^{n} \frac{1}{2} e_{i,a}^2 + \frac{1}{2} u_{min}{}^2$.

According to Young's inequality and **Lemma** 3, it can be obtained that

$$\begin{aligned}\tfrac{\sigma_1}{\gamma} \tilde{\theta} \hat{\theta} =& -\tfrac{\sigma_1}{\gamma} \tilde{\theta}^2 + \tfrac{\sigma_1}{\gamma} \tilde{\theta} \theta \\ \leq& -\sigma_1 (\tfrac{\tilde{\theta}^2}{2\gamma})^p + \sigma_1 (1-p) p^{\frac{p}{1-p}} + \tfrac{\sigma_1}{2\gamma} \theta^2.\end{aligned} \quad (40)$$

By applying **Lemmas** 2 and 3, we can infer that

$$\tfrac{\sigma_2}{\gamma} \tilde{\theta} \hat{\theta}^{2q} \leq 2^{2q-2} \tfrac{\sigma_2}{\gamma} \tfrac{2q-1}{2q} (\theta^{2q} - \tilde{\theta}^{2q}). \quad (41)$$

Substituting Eqs(40) and (41) into Eq.(39), $\dot{V}_n$ becomes

$$\begin{aligned}\dot{V}_n \leq& - \sum_{i=1}^{n} (c_{i,1} e_i^{2p} + c_{i,2} e_i^{2q}) - \sigma_1 (\tfrac{\tilde{\theta}^2}{2\gamma})^p \\ &+ \sigma_1 (1-p) p^{\frac{p}{1-p}} + \tfrac{\sigma_1}{2\gamma} \theta^2 + b_n \\ &+ 2^{2q-2} \tfrac{\sigma_2}{\gamma} \tfrac{2q-1}{2q} (\theta^{2q} - \tilde{\theta}^{2q}) \\ \leq& -c_1 \sum_{i=1}^{n} (\tfrac{e_i^2}{2})^p - c_2 \sum_{i=1}^{n} (\tfrac{e_i^2}{2})^q - \sigma_1 (\tfrac{\tilde{\theta}^2}{2\gamma})^p \\ &- 2^{2q-2} \sigma_2 \tfrac{2q-1}{q} (2\gamma)^{2q-1} (\tfrac{\tilde{\theta}^2}{2\gamma})^q + \underline{b}_n,\end{aligned} \quad (42)$$

where $\underline{b}_n = \sigma_1 (1-p) p^{\frac{p}{1-p}} + \frac{\sigma_1}{2\gamma} \theta^2 + 2^{2q-2} \frac{\sigma_2}{\gamma} \frac{2q-1}{2q} \theta^{2q} + b_n$, $c_1 = 2^p \min\{c_{1,1},\ c_{2,1},\ ...c_{n,1}\}$, and $\underline{c}_2 = 2^q \min \{c_{1,2},\ c_{2,2},\ ....\ c_{n,2}\}$. This yields from **Lemma** 3 that

$$[\sum_{i=1}^{n} \frac{e_i^2}{2} + \frac{\tilde{\theta}^2}{2\gamma}]^p \leq \sum_{i=1}^{n} (\frac{e_i^2}{2})^p + (\frac{\tilde{\theta}^2}{2\gamma})^p, \quad (43)$$

$$(n+1)^{1-q} [\sum_{i=1}^{n} \frac{e_i^2}{2} + \frac{\tilde{\theta}^2}{2\gamma}]^q \leq \sum_{i=1}^{n} (\frac{e_i^2}{2})^q + (\frac{\tilde{\theta}^2}{2\gamma})^q. \quad (44)$$

Combining Eqs(43) and (44) with Eq.(42) leads to

$$\begin{aligned}\dot{V}_n \leq& -\underline{c}_1 [\sum_{i=1}^{n} \tfrac{e_i^2}{2} + \tfrac{\tilde{\theta}^2}{2\gamma}]^p + \underline{b}_n \\ &- \underline{c}_2 (n+1)^{1-q} [\sum_{i=1}^{n} \tfrac{e_i^2}{2} + \tfrac{\tilde{\theta}^2}{2\gamma}]^q \\ \leq& -\underline{c}_1 V_n{}^p - \bar{c}_2 V_n{}^q + \underline{b}_n,\end{aligned} \quad (45)$$

where $\underline{c}_1 = \min\{c_1, \sigma\}$ and $\bar{c}_2 = \underline{c}_2 (n+1)^{1-q}$ with $\underline{c}_2 = \min\{c_2, 2^{2q-2} \sigma_2 \frac{2q-1}{q} (2\gamma)^{2q-1}\}$.

So far, we have accomplished the design process of practical fixed time adaptive control for uncertain nonlinear systems (1).

**Remark 4.** According to **Definition** 1 and property (8) of $\zeta_i$, if the function $\zeta_1$ can follow the signal $\alpha_{1,f}$ within a desired error region, then we can deduce that the virtual control signal $\alpha_{i,f}$ is nonconstrained. Thus, compared with the BLF-based methods, the feasibility condition of virtual control signals is fully removed.

### 3.3 Stability Analysis

On the basis of the above derived formulation, the primary results summarized by **Theorem 1** are shown as follows.

**Theorem 1.** Consider uncertain nonlinear systems (1) subject to time-varying asymmetric state constraints (2) and quantized input (3) satisfying **Assumptions 1** and **2**. By designing the virtual control signals Eqs(20) and (27), the practical fixed-time adaptive controller Eq.(35) and the adaptive laws Eq.(38), we can get the following results:

(1)The boundedness of all signals in the closed-loop system (1) can be achieved.

(2)The time-varying asymmetric constraints (2) on system states are not overstepped, and the feasibility check is avoided.

(3)The output signal will follow the desired signal within a small error interval in predetermined time $T$, and $T$ can be computed using **Lemma** 1.

**Proof**: First, for convenience, define $V(s) = V_n\big(e_1, ..., e_n, \tilde{\theta}\big)$ and $s = \big[e_1, ..., e_n, \tilde{\theta}\big]$. Achieving the process of fixed time stability of closed-loop systems can be separated into two situations.

**Situation 1**: If $V(s) > 1$ and $\underline{b}_n$ satisfy $\underline{b}_n < min\big\{(1-\xi)\underline{c}_1, (1-\xi)\bar{c}_2\big\}$ $(0 < \xi < 1)$, we can deduce the following inequalities

$$\dot{V}(s) \leq -\bar{c}_2 V^q(s) + \underline{b}_n. \tag{46}$$

$$\frac{\underline{b}_n}{(1-\xi)\bar{c}_2} \leq 1 \leq V(s). \tag{47}$$

$$\underline{b}_n \leq (1-\xi)\bar{c}_2 V^q(s). \tag{48}$$

Combining Eqs(46) and (48), one has

$$\dot{V}(s) \leq -\xi\bar{c}_2 V^q(s), \tag{49}$$

which implies that

$$\int_0^t \frac{\dot{V}(s)}{V^q(s)} dt \leq -\xi \int_0^t \bar{c}_2 dt. \tag{50}$$

By calculating Eq.(50), one gets

$$\frac{1}{1-q} V^{1-q}(s(t)) - \frac{1}{1-q} V^{1-q}(s(0)) \leq -\xi\bar{c}_2 t. \tag{51}$$

Then we can derive that $V^{q-1}(s(t)) \leq \frac{1}{\xi\bar{c}_2 t(q-1)}$. In addition, by defining $T_1 = \frac{1}{\xi\bar{c}_2(q-1)}$, it can be determined that for $\forall t \geq T_1$, we have $V^{q-1}(s(t)) \leq 1$ and $V(s(t)) \leq 1$.

**Situation 2**: If $V(s) \leq 1$, one has

$$\dot{V}(s) \leq -\xi\underline{c}_1 V^p(s) - (1-\xi)\underline{c}_1 V^p(s) + \underline{b}_n. \tag{52}$$

Define $\Xi_s = \big\{s | V^p(s) \leq \frac{\underline{b}_n}{(1-\xi)\underline{c}_1}\big\}$ and $\bar{\Xi}_s = \big\{s | V^p(s) > \frac{\underline{b}_n}{(1-\xi)\underline{c}_1}\big\}$.

**(1)** If $s(t) \in \bar{\Xi}_s$, according to Eq.(52), we have

$$\dot{V}(s) \leq -\xi\underline{c}_1 V^p(s), \tag{53}$$

which means that

$$\int_{t_0}^t \frac{\dot{V}(s)}{V^p(s)} dt \leq -\xi \int_{t_0}^t \underline{c}_1 dt. \tag{54}$$

Computing Eq.(54) yields that

$$\frac{1}{1-p} V^{1-p}(s(t)) - \frac{1}{1-p} V^{1-p}(s(t_0)) \leq -\xi\underline{c}_1(t-t_0) \tag{55}$$

Based on **Situation 1**, we have $V(s(t_0)) \leq 1$ for $t_0 \geq T_1$. Thus, it can be achieved that $V^{1-p}(s(t)) \leq 1 - \xi\underline{c}_1(1-p)(t-t_0)$. By defining $T_2 \geq \frac{1}{\xi\underline{c}_1(1-p)}$ and considering the positive definite property of $V(s)$, we can obtain that $V^p(s) \leq \frac{\underline{b}_n}{\underline{c}_1(1-\xi)}$ for $\forall t \geq t_0 + T_2$.

**(2)** If $s(t) \in \Xi_s$, considering LaSalle's invariance principle, it is true that $s(t)$ didn't violate the set $\Xi_s$. Based on the aforementioned analysis, because $\Xi_z$ is an invariant set, we can find that $V^p(s) \leq \frac{\underline{b}_n}{\underline{c}_1(1-\xi)}$ is true for $\forall t \geq T_1 + T_2$. Moreover, in light of **Lemma** 1, we have $\|s\| \leq \beta^{-1}(\frac{\underline{b}_n}{(1-\xi)\underline{c}_1})^{\frac{1}{p}}$. Therefore, the control systems (1) can achieve stability in fixed time, and the settling time $T$ satisfies $T \leq \frac{1}{\xi\underline{c}_1(1-p)} + \frac{1}{\xi\bar{c}_2(q-1)}$.

Furthermore, we prove that all states with constraints have not overstepped their constraints. Defining a parameter $P = \min\{\underline{c}_1,\ \bar{c}_2\}$ and combining **Lemma** 5, $\dot{V}_n$ can be simplified as

$$\dot{V}_n \leq -PV_n + \underline{b}_n. \tag{56}$$

By multiplying both sides by $e^{Pt}$ yields $\frac{d(V_n e^{Pt})}{dt} \leq \underline{b}_n e^{Pt}$. Meanwhile, integrating both sides results in

$$V_n(t) \leq V_n(0) + \frac{\underline{b}_n}{P}. \tag{57}$$

From **Lemma** 4 and inequality Eq.(57), the boundedness of $V_n(t)$ can be determined. According to the definition of $V_n(t)$, it can be found that $e_i$ and $\tilde{\theta}$ are bounded. Noted that $\alpha_{1,f} \in L_\infty$ in the compact set $U_d$ and $e_1 = \zeta_1 - \alpha_{1,f}$, it is guaranteed that $\zeta_1 \in L_\infty$. Thus, we can infer that the state $x_1$ remains in the interval $U_1$ formed by the constraint functions $k_{1l}(t)$ and $k_{1h}(t)$ under the initial condition $x_1(0) \in U_1$, which means that $x_1$ does not overstep the time-varying asymmetric constraints. Similarly, the boundedness of $\zeta_i$, $\alpha_{i,f}$ and $u$ can be obtained, while we can conclude that the constraint areas of system state $x_i$ are not violated.

Finally, we will prove that the real tracking error $z = x_1 - y_d$ is bounded. By calculating, we can obtain $z = \frac{e_1}{\varrho}$, where $\varrho = \frac{\overline{k}_{1l} - k_{1l}}{(x_1 - k_{1l})(y_d - k_{1l})} + \frac{k_{1h} - \underline{k}_{1h}}{(k_{1h} - x_1)(k_{1h} - y_d)}$. Note that $x_1 \subset U_1$ and $y_d \in U_d \subset U_1$, which implies that there exist two positive constants $\overline{\nu}_j$ and $\underline{\nu}_j$, $(j = 1, 2)$, such that inequalities $0 < \underline{\nu}_1 \leq (x_1 - k_{1l})(y_d - k_{1l}) \leq \overline{\nu}_1$ and $0 < \underline{\nu}_2 \leq (k_{1h} - x_1)(k_{1h} - y_d) \leq \overline{\nu}_2$ hold. This proves that the boundedness of $\varrho$. Therefore, there exist two constants, $\underline{\varrho}$ and $\overline{\varrho}$, satisfying $0 < \underline{\varrho} \leq \varrho \leq \overline{\varrho}$, so it follows that $z$ is bounded. Meanwhile, the inequality Eq.(56) can be rewritten as $\dot{V}_n(t) \leq -Pe_1{}^2 + \underline{b}_n$, which indicates that $\dot{V}_n(t)$ will be negative if $|e_1| > \sqrt{\frac{\underline{b}_n}{P}}$. Thus, it can be obtained that $e_1$ enters into and remains within the compact set $\Psi_{e1} = \left\{ e_1 \in R \big| |e_1| \leq \sqrt{\frac{\underline{b}_n}{P}} \right\}$. In addition, we can further find that the real tracking error $z$ accesses and remains within the compact set $\Psi_z = \left\{ z \in R \big| |z| \leq \frac{1}{\underline{\varrho}} \sqrt{\frac{\underline{b}_n}{P}} \right\}$. Obviously, the tracking error can converge to a small range around zero in a predefined time by choosing an appropriate parameter $P$. The proof is completed.

## 4 SIMULATION EXAMPLE

In this section, two examples, an example of numerical simulation and an example of practical application, are provided to verify the availability of the proposed control strategy.

### 4.1 Numerical Comparisons Example

In this subsection, the method presented in this paper would be compared with the BLF-based method in (Li,2020). We take the following nonlinear system model into account:

$$\begin{cases} x_1 = f_1(\bar{x}_2) + x_2, \\ x_2 = f_2(\bar{x}_2) + g(\bar{x}_2)\, q(u), \\ y = x_1, \end{cases} \tag{58}$$

where $f_1(\bar{x}_2) = x_1{}^2 x_2 + 0.1\cos(0.5x_1)$, $f_2(\bar{x}_2) = x_1 + 0.1x_2 + 0.5\sin(x_2)$ and $g(\bar{x}_2) = 0.2\cos(x_1 x_2) + 1$. The desired signal is selected as $y_d = \sin(0.5t) + 0.5\cos(t)$, which satisfies **Assumption 2**. The system states are required to be maintained in the following areas

$$x_i \in U_i := \{(t, x_i) \in (R_+ \times R)| \\ k_{il}(t) < x_i < k_{ih}(t), k_{il} \in R, k_{ih} \in R\}, \tag{59}$$

where $k_{1h}(t) = -\sin(t) + \cos(t) + 6$, $k_{1l}(t) = 0.5\sin(t) - 6$, $k_{2h}(t) = -0.2\sin(t) + 0.4\cos(t) + 6$, $k_{2l}(t) = -\sin(t) + \cos(t) - 6$. According to **Theorem 1**, the first-order filter, the virtual control signals, the adaptive laws, and the controllers are constructed as Eqs(13), (20), and (27), and Eqs(38) and (35), respectively. The related parameters in this work are set to $c_{11} = c_{12} = c_{21} = c_{22} = 2$, $k_1 = k_2 = 70$, $a_1 = a_2 = 5$ , $\sigma_1 = \sigma_2 = \gamma = 5$, $\tau_1 = 0.001$, $\overline{k}_{1h} = \underline{k}_{1l} = -2$, $\overline{k}_{2h} = \underline{k}_{2l} = -2$, $p = 0.5$, $q = 3$, $\lambda = 0.3$, $u_{min} = 2$. The different parameters of the method in (Li,2020) are set to $\sigma_1 = 10e^{-2t}$, $\sigma_2 = 15e^{-0.01t}$, $k_{a1} = k_{b1} = k_{a2} = k_{b2} = -2$, and the remaining parameters are the same as those in this work. The initial conditions for both are selected as $x_1(0) = 0.3$, $x_2(0) = 0.2$, and $\theta(0) = 2$.

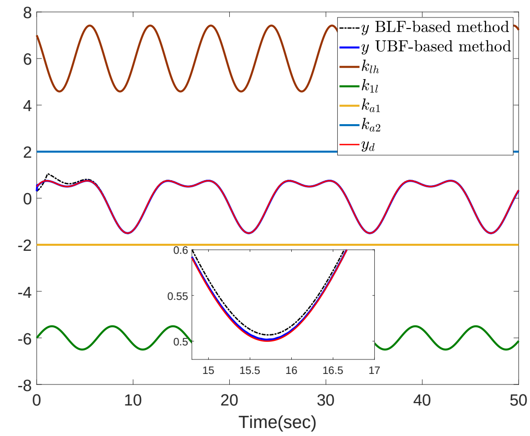

**Fig. 3 The comparison of tracking trajectories after using the two methods.**

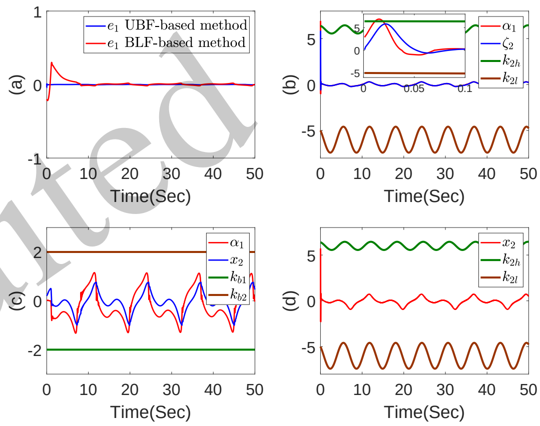

**Fig. 4 (a) Tracking errors of two methods. (b) $\zeta_2$ and $\alpha_1$ under UBF-based method. (c) $x_2$ and $\alpha_1$ under BLF-based method. (d) $x_2$ under UBF-based method.**

The comparative results are shown in **Figs** 3 and 4. Obviously, from **Fig.** 3, the UBF-based method proposed in this paper enables the system to obtain better tracking capabilities compared with the

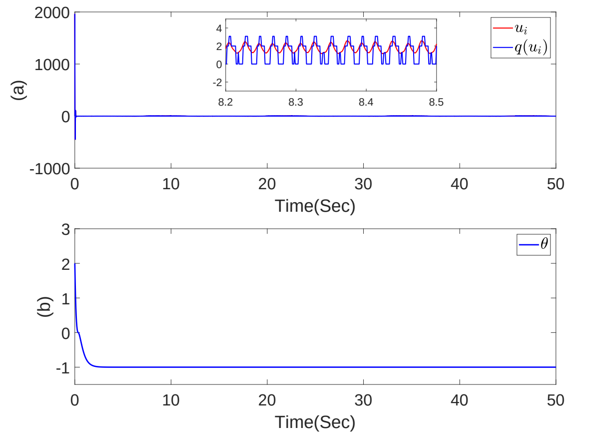


**Fig. 5 (a)** $q(u_i)$ **and** $u_i$ **for Eq.**(58)**. (b)** $\theta$ **for Eq.**(58)**.**

BLF-based method in (Li,2020). In addition, the detailed comparisons are illustrated in **Fig.** 4. The tracking errors for the two methods are exhibited in **Fig.** 4(a). In **Figs** 4(b) and 4(c), the differences in virtual control signals are demonstrated, where the virtual control signal can surpass state constraints in **Fig.** 4(b), but the system state still obeys the state constraints in **Fig.** 4(d) under the UBF-based method. In **Fig.** 4(c), under the BLF-based method in (Li,2020), the virtual control signal $\alpha_1$ and the system state $x_2$ have not violated the state constraints. The quantization input $q(u_i)$ and the system input $u_i$ are displayed in **Fig.** 5(a). The adaptive laws are plotted in **Fig.** 5(b).

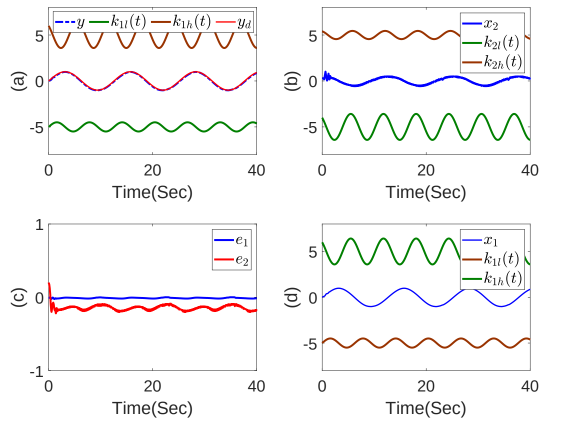


**Fig. 6 (a) Tracking trajectories for Eq.**(61)**. (b)** $x_2$ **and its constraint functions for Eq.**(61)**. (c) Tracking errors for Eq.**(61)**. (d)** $x_1$ **and its constraint functions for Eq.**(61)**.**

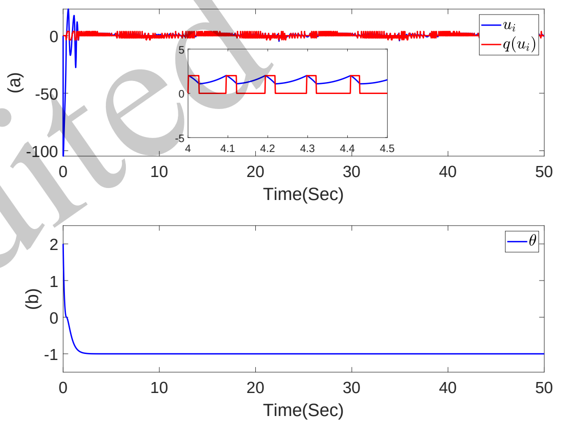


**Fig. 7 (a)** $q(u_i)$ **and** $u_i$ **for Eq.**(61)**. (b)** $\theta$ **for Eq.**(61)**.**



### 4.2 Practical Example

In this subsection, we introduce a ship control problem described in (Xing et al.,2017) as a practical example to illustrate the validity of the proposed method, which is modeled mathematically as follows

$$\ddot{y} + \Phi\dot{y} + b_0({Mx_1}^3 + Lx_1) = b_0 q(u_i), \qquad (60)$$

where $b_0 \neq 0$ denotes a constant, $q(u_i)$ expresses the quantized input, and $y$ represents the course angular velocity of the ship. $L$ and $M$ are the unknown constants, which are related to the hydrodynamic coefficients and the mass of the ship. By setting $x_1 = y$ and $x_2 = \dot{x}_1$, the systems (60) can be rewritten as

$$\begin{cases} \dot{x}_1 = x_2 \\ \dot{x}_2 = -\Phi x_2 - b_0(Mx_1^3 + Lx_1) + b_0 q(u_i) \end{cases} \qquad (61)$$

Let $\Phi = -0.1$, $b_0 = 1$, $M = 0.7$, $L = 0.4$, then we can derive that $f_1(x_1, x_2) = 0$, $f_2(x_1, x_2) = -0.1\ x_2 - 0.4x_1 - 0.7x_1^2$ and $g(x_1, x_2) = 1$. The upper and the lower bound function of states $x_1$ and $x_2$ are set as $k_{1h} = 0.5\sin(t) + 5$, $k_{2h} = -\sin(t) + \cos(t) + 5$ and $k_{1l} = -\sin(t) + \cos(t) - 5$, $k_{2l} = -0.2\sin(t) + 0.4\cos(t) - 5$, respectively. Meanwhile, some relevant parameter values are chosen as $a_2 = 10$, $k_1 = 60$, $k_2 = 60$, $c_{11} = 5$, $c_{12} = 5$, $c_{21} = 15$, $c_{22} = 15$, $\gamma = 10$, $\sigma_1 = 5$, $\sigma_2 = 5$, $\delta = 0.05$, $\lambda = 0.1$, $u_{min} = 2$, $\underline{k}_{1h} = 2$, $\underline{k}_{2h} = 2$, $\overline{k}_{1l} = -2$, $\overline{k}_{2l} = -2$, $\tau = 0.25$. The initial values of the controlled systems are selected as $x_1(0) = 0$, $x_2(0) = 0.3$, and $\theta(0) = 2$. The desired trajectories are provided by $y_d(t) = \sin(0.5t)$.

**Figs** 6 and 7 provide the relevant simulation results. The tracking performance is shown in **Fig.** 6(a) and the tracking errors are given in **Fig.** 6(c). The system states are exhibited in **Figs** 6(d) and 6(b), where the system states $x_1$ and $x_2$ have not overstepped their state constraints. **Fig.** 7(a) shows the quantized input and the input signal. The trajectory of adaptive law is exhibited in **Fig.** 7(b).

## 5 CONCLUSION

In this technical note, we researched the issue of adaptive tracking control for a class of uncertain nonlinear systems with input quantization and time-varying asymmetric constraints. On the basis of the UBF method, a practical fixed time adaptive fuzzy control strategy has been developed, which guarantees that the time-varying asymmetric state constraints are not overstepped and removes the feasibility condition of virtual control signals. By introducing the command filter method, the "explosion of complexity" issue has been addressed. FLSs have been applied to approximate unknown nonlinear functions. According to the practical fixed time Lyapunov stability criterion, it has been demonstrated that the tracking error will converge to an expected range around zero in a predetermined time. The effectiveness of the proposed strategy is illuminated using a simulation example.

## Acknowledgments

This research work was funded by Institutional Fund Projects under grant no. (IFPIP: 131-611-1443). The authors gratefully acknowledge technical and financial support provided by the Ministry of Education and King Abdulaziz University, DSR, Jeddah, Saudi Arabia.

## Contributors

**Zixuan Huang**: Ideas, Formulation or evolution of overarching research goals and aims, Writing original draft preparation. **Huanqing Wang** and **Ben Niu**: Oversight and leadership responsibility for the research activity planning and execution, including mentorship external to the core team. **Xudong Zhao** : Coordination for the research activity planning, including language and grammar checks. **Adil M. Ahmad**: Conceptualization, Visualization.

## Compliance with ethics guidelines

Zixuan Huang, Huanqing Wang, Ben Ni, Xudong Zhao and Adil M. Ahmad declare that they have no conflict of interest.

## Data availability

The data that support the findings of this study are available from the corresponding author upon reasonable request.



## References

Bhat SP, Bernstein DS, 1998. Continuous finite-time stabilization of the translational and rotational double integrators. *IEEE Transactions on automatic control*, 43(5):678-682. https://doi.org/10.1109/9.668834

Chen B, Liu X, Liu K, et al., 2013. Adaptive fuzzy tracking control of nonlinear mimo systems with time-varying delays. *Fuzzy Sets and Systems*, 217:1-21. https://doi.org/10.1016/j.fss.2012.11.002

Chen W, Li J, 2010. Globally decentralized adaptive backstepping neural network tracking control for unknown nonlinear interconnected systems. *Asian Journal of Control*, 12(1):96-102. https://doi.org/10.1002/asjc.160

Gao Z, Liu D, Qian M, 2022. Decentralised adaptive tracking control for the interconnected nonlinear systems with asymmetric full state dynamic constraints. *International Journal of Control*, 95(10):2840-2853. https://doi.org/10.1080/00207179.2021.1939421

Guo S, Zhao X, Wang H, et al., 2023. Distributed consensus of heterogeneous switched nonlinear multiagent systems with input quantization and dos attacks. *Applied Mathematics and Computation*, 456:128127. https://doi.org/10.1016/j.amc.2023.128127

Hou H, Yu X, Xu L, et al., 2020. Finite-time continuous terminal sliding mode control of servo motor systems. *IEEE Transactions on Industrial Electronics*, 67(7):5647-5656. https://doi.org/10.1016/j.automatica.2013.08.003

Huang J, Wang W, Wen C, et al., 2018. Adaptive control of a class of strict-feedback time-varying nonlinear systems with unknown control coefficients. *Automatica*, 93:98-105. https://doi.org/10.1016/j.automatica.2018.03.061

Huang S, Zong G, Wang H, et al., 2023. Command filter-based adaptive fuzzy self-triggered control for mimo nonlinear systems with time-varying full-state constraints. *International Journal of Fuzzy Systems*,. https://doi.org/10.1007/s40815-023-01560-8

Kim BS, Yoo SJ, 2015. Adaptive control of nonlinear pure-feedback systems with output constraints: integral barrier lyapunov functional approach. *International Journal of Control, Automation and Systems*, 13(1):249-256. https://doi.org/10.1007/s12555-014-0018-3

Li J, Yang Y, Hua C, et al., 2017. Fixed-time backstepping control design for high-order strict-feedback non-linear systems via terminal sliding mode. *IET Control Theory & Applications*, 11(8):1184-1193. https://doi.org/10.1049/iet-cta.2016.1143

Li S, Wang X, 2013. Finite-time consensus and collision avoidance control algorithms for multiple auvs. *Automatica*, 49(11):3359-3367. https://doi.org/10.1016/j.automatica.2013.08.003

Li Y, Tong S, 2016. Adaptive fuzzy output constrained control design for multi-input multioutput stochastic nonstrict-feedback nonlinear systems. *IEEE Transactions on Cybernetics*, 47(12):4086-4095. https://doi.org/10.1109/TCYB.2016.2600263

Li YX, 2019. Finite time command filtered adaptive fault tolerant control for a class of uncertain nonlinear systems. *Automatica*, 106:117-123. https://doi.org/10.1016/j.automatica.2019.04.022

Li YX, 2020. Barrier lyapunov function-based adaptive asymptotic tracking of nonlinear systems with unknown virtual control coefficients. *Automatica*, 121:109181. https://doi.org/10.1016/j.automatica.2020.109181

Liu S, Niu B, Zong G, et al., 2023. Adaptive neural dynamic-memory event-triggered control of high-order random nonlinear systems with deferred output constraints. *IEEE Transactions on Automation Science and Engineering*, :1-13. https://doi.org/10.1109/TASE.2023.3269509

Liu Y, Tong S, 2017. Barrier lyapunov functions for nussbaum gain adaptive control of full state constrained nonlinear systems. *Automatica*, 76:143-152. https://doi.org/10.1016/j.automatica.2016.10.011

Ma H, Liang H, Zhou Q, et al., 2018. Adaptive dynamic surface control design for uncertain nonlinear strict-feedback systems with unknown control direction and disturbances.,. *IEEE Transactions on Systems, Man, and Cybernetics: Systems*, 49(3):506-515. https://doi.org/10.1109/TSMC.2018.2855170

Ni J, Liu L, Liu C, et al., 2016. Fast fixed-time nonsingular terminal sliding mode control and its application to chaos suppression in power system. *IEEE Transactions on Circuits and Systems II: Express Briefs*, 64(2):151-155. https://doi.org/10.1109/TCSII.2016.2551539

Polyakov A, 2011. Nonlinear feedback design for fixed-time stabilization of linear control systems. *IEEE Transactions on Automatic Control*, 57(8):2106-2110. https://doi.org/10.1109/TAC.2011.2179869

Shi Y, Shao X, Zhang W, 2020. Quantized learning control for flexible air-breathing hypersonic vehicle with limited actuator bandwidth and prescribed performance. *Aerospace Science and Technology*, 97:105629. https://doi.org/10.1016/j.ast.2019.105629

Sui S, Tong S, 2018. Observer-based adaptive fuzzy quantized tracking dsc design for mimo nonstrict-feedback nonlinear systems. *Neural Computing and Applications*, 30:3409-3419. https://doi.org/10.1007/s00521-017-2929-4

Sun ZY, Liu CY, Su SF, et al., 2019. Robust stabilization of high-order nonlinear systems with unknown sensitivities and applications in humanoid robot manipulation. *IEEE Transactions on Systems, Man, and Cybernetics: Systems*, 51(4):2370-2381. https://doi.org/10.1109/TSMC.2019.2931768

Swaroop D, Hedrick JK, Yip PP, et al., 2000. Dynamic surface control for a class of nonlinear systems. *IEEE transactions on automatic control*, 45(10):1893-1899. https://doi.org/10.1109/TAC.2000.880994

Tang ZL, Ge SS, Tee KP, et al., 2016. Robust adaptive neural tracking control for a class of perturbed uncertain nonlinear systems with state constraints. *IEEE Transactions on Systems, Man, and Cybernetics: Systems*, 46(12):1618-1629. https://doi.org/10.1109/TSMC.2015.2508962

Tee KP, Ge SS, 2011. Control of nonlinear systems with partial state constraints using a barrier lyapunov function. *International Journal of Control*, 84(12):2008-2023. https://doi.org/10.1080/00207179.2011.631192

Tee KP, Ge SS, Tay EH, 2009. Barrier lyapunov functions for the control of output-constrained nonlinear systems. *Automatica*, 45(4):918-927. https://doi.org/10.1016/j.automatica.2008.11.017

Wang F, Lai G, 2020. Fixed-time control design for nonlinear uncertain systems via adaptive method. *Systems & Control Letters*, 140:104704. https://doi.org/10.1016/j.sysconle.2020.104704

Wang H, Chen B, Liu X, et al., 2013. Robust adaptive fuzzy tracking control for pure-feedback stochastic nonlinear systems with input constraints. *IEEE Transactions on Cybernetics*, 43(6):2093-2104. https://doi.org/10.1109/TCYB.2013.2240296

Wang S, Xia J, Park JH, et al., 2021. Adaptive event-triggered control for mimo nonlinear systems with asymmetric state constraints based on unified barrier functions. *International Journal of Robust and Nonlinear Control*, 31(18):9397-9415. https://doi.org/10.1002/rnc.5776

Wang T, Zhang Y, Qiu J, et al., 2014. Adaptive fuzzy backstepping control for a class of nonlinear systems with sampled and delayed measurements. *IEEE Transactions on Fuzzy Systems*, 23(2):302-312. https://doi.org/10.1109/TFUZZ.2014.2312026

Xing L, Wen C, Liu Z, et al., 2017. Robust adaptive output feedback control for uncertain nonlinear systems with quantized input. *International Journal of Robust and Nonlinear Control*, 27(11):1999-2016. https://doi.org/10.1002/rnc.3669

Xu B, Liang Y, Li YX, et al., 2022. Adaptive command filtered fixed-time control of nonlinear systems with input quantization. *Applied Mathematics and Computation*, 427(15):127186. https://doi.org/10.1016/j.amc.2022.127186

Yu S, Yu X, Shirinzadeh B, et al., 2005. Continuous finite-time control for robotic manipulators with terminal sliding mode. *Automatica*, 41(11):1957-1964. https://doi.org/10.1016/j.automatica.2005.07.001

Zhang L, Liang H, Sun Y, et al., 2019. Adaptive event-triggered fault detection scheme for semi-markovian jump systems with output quantization. *IEEE Transactions on Systems, Man, and Cybernetics: Systems*, 51(4):2370-2381. https://doi.org/10.1109/TSMC.2019.2912846

Zhao H, Wang H, Xu N, et al., 2023. Fuzzy approximation-based optimal consensus control for nonlinear multiagent systems via adaptive dynamic programming. *Neurocomputing*, 553:126529. https://doi.org/10.1016/j.neucom.2023.126529

Zhao K, Song Y, Chen CP, et al., 2020. Control of nonlinear systems under dynamic constraints: A unified barrier function-based approach. *Automatica*, 119:109102. https://doi.org/10.1016/j.automatica.2020.109102

Zuo Z, Tian B, Defoort M, et al., 2017. Fixed-time consensus tracking for multiagent systems with high-order integrator dynamics. *IEEE Transactions on Automatic Control*, 63(2):563-570. https://doi.org/10.1109/TAC.2017.2729502